RSC Advances

PAPER

View Article Online
View Journal | View Issue

Check for updates

Cite this: *RSC Adv.*, 2018, **8**, 37740

Interaction mechanism between TiO_2 nanostructures and bovine leukemia virus proteins in photoluminescence-based immunosensors

Alla Tereshchenko,*[ab] Valentyn Smyntyna[a] and Arunas Ramanavicius *[b]

In this research a mechanism of interaction between a semiconducting TiO_2 layer and bovine leukemia virus protein *gp*51, applied in the design of photoluminescence-based immunosensors, is proposed and discussed. Protein *gp*51 was adsorbed on the surface of a nanostructured TiO_2 thin film, formed on glass substrates (TiO_2/glass). A photoluminescence (PL) peak shift from 517 nm to 499 nm was observed after modification of the TiO_2/glass by adsorbed *gp*51 (*gp*51/TiO_2/glass). After incubation of the *gp*51/TiO_2/glass in a solution containing anti-*gp*51, a new structure (anti-*gp*51/*gp*51/TiO_2/glass) was formed and the PL peak shifted backwards from 499 nm to 516 nm. The above-mentioned PL shifts are attributed to the variations in the self-trapped exciton energy level, which were induced by the changes of electrostatic interaction between the adsorbed *gp*51 and the negatively charged TiO_2 surface. The strength of the electric field affecting the photoluminescence centers, was determined from variations between the PL-spectra of TiO_2/glass, *gp*51/TiO_2/glass and anti-*gp*51/*gp*51/TiO_2/glass. The principle of how these electric field variations are induced has been predicted. The highlighted origin of the changes in the photoluminescence spectra of TiO_2 after its protein modification reveals an understanding of the interaction mechanism between TiO_2 and proteins that is the key issue responsible for biosensor performance.

Received 3rd September 2018
Accepted 24th October 2018

DOI: 10.1039/c8ra07347c

rsc.li/rsc-advances

Open Access Article. Published on 09 November 2018. Downloaded on 11/20/2018 8:42:53 AM.
This article is licensed under a Creative Commons Attribution-NonCommercial 3.0 Unported Licence.

1. Introduction

Bovine leukemia is a lethal retroviral infection, which is induced by bovine leukemia virus (BLV). There is a significant risk that BLV can infect the other mammalians as in the case of other retroviruses' – such as, human immunodeficient virus (HIV). Therefore outbreaks of this infectious disease can significantly damage the ecosystem. For this reason the development of advanced bioanalytical systems for the determination of biomarkers of BLV-infection are required.[1,2] Among many different immunosensors, the photoluminescence-based (PL) immunosensors seems to be the most promising for the improvement in diagnosis of virus induced diseases. In PL-immunosensors nanostructured ZnO or TiO_2 can be used as very efficient photoluminescence transducers.[3,4] TiO_2 and its composites are extensively used as wide-band gap semiconductors with a unique combination of physical and chemical properties.[5–7]

A good biocompatibility of TiO_2 nanostructures, their applicability at physiological pHs in the range of ~5.5–7.0, non-toxicity and excellent chemical stability have resulted in the extensive application of TiO_2 in electrochemical,[8–10] electrical[11] and optical[12–14] biosensors. Optical biosensors are increasingly studied class of biosensors because they allow to evaluate some inter-molecular interactions contactless[15] and without any chemical/physical labels.[3] The development of immunosensors, based on the optical detection methods, that can be applied for the determination of large variety of analytes in the complex biological samples[7,12,14,15] is of great interest.

Nanostructured TiO_2 is known as a material of intense photoluminescence at room temperature.[16,17] The application of TiO_2 photoluminescence properties in optical biosensors and immunosensors have been reported in the range of works. The changes in the photoluminescence spectra (shift of PL-maximum and the variation of PL-signal intensity) were exploited as analytical signals for the determination of target analyte.[18,19] However the interaction mechanism of proteins with TiO_2 and the origin of the changes in the photoluminescence spectra were not discussed, although the mechanism of the interaction between semiconductor and proteins is the key in solving many of problems, which are still arising during the development of TiO_2-based immunosensors, such as an improvement of sensitivity and selectivity.[3,13,14]

This work is aiming to highlight the origin of the changes in the photoluminescence spectra of TiO_2 resulted after the protein adsorption on its surface during the formation of biosensitive

[a]*Experimental Physics Department, Faculty of Mathematics, Physics and Information Technologies, Odesa National I.I. Mechnikov University, Pastera 42, 65023, Odesa, Ukraine*

[b]*Department of Physical Chemistry, Institute of Chemistry, Faculty of Chemistry and Geosciences, Vilnius University, Naugarduko 24, LT-03225 Vilnius, Lithuania. E-mail: Arunas.Ramanavicius@chf.vu.lt; alla_teresc@onu.edu.ua*

This journal is © The Royal Society of Chemistry 2018

Open Access Article. Published on 09 November 2018. Downloaded on 11/20/2018 8:42:53 AM.
This article is licensed under a Creative Commons Attribution-NonCommercial 3.0 Unported Licence.

layer and after the interaction of biosensitive layer with the analyte. As it is proposed, the reason of the PL shifts observed after modification of TiO_2/glass by *gp*51 proteins is an electrostatic interaction between adsorbed *gp*51 and negatively charged TiO_2 surface. The strength of the electric field affecting photoluminescence centers, localized close to the surface of TiO_2/glass, is determined from variations of the PL-spectra of TiO_2/glass, *gp*51/TiO_2/glass and anti-*gp*51/*gp*51/TiO_2/glass. The principle of how these electric field variations are induced is discussed. The influence of several important parameters, including charge density of charged atoms/groups/domains in the specific binding biomolecules, effective coverage area by specific binding biomolecules and variation of the potential barrier are taken into account during the elaboration of the model.

2. Materials and methods

2.1. Formation and characterization of TiO_2 samples

Nanostructured TiO_2 layers containing TiO_2 nanoparticles were formed on the glass substrates (TiO_2/glass) by the deposition of colloidal suspension of TiO_2 nanoparticles (Sigma Aldrich, 99.7%, particle size of 32 nm), dissolved in ethanol. Initial concentration of TiO_2 nanoparticles was about 0.01 mg ml^{-1}. The formed TiO_2/glass structures were dried at room temperature and then annealed at 350 °C. Structural and surface characterization of the obtained samples showed that in TiO_2/glass structures the TiO_2 kept the anatase structure and TiO_2 nanoparticles formed a high surface area porous structure, which was suitable for the formation of biosensitive layer. More detailed description of deposition and characterization procedures, which were applied for the characterization of nanostructured TiO_2/glass layers is reported in earlier our researches.[18,19]

Optical characterization of the nanostructured TiO_2/glass layers was performed by photoluminescence measurements using 355 nm solid state laser as the excitation source. Optical setup is described in detail in previous our researches.[19,20] The PL-spectra were recorded in the range of wavelength from 360 to 800 nm.

2.2. Fabrication and evaluation of an immunosensor

The immobilization of biological molecules was carried out by incubation in a solution containing leukemia virus proteins – *gp*51, similar to the immobilization procedure described in earlier works.[18–20] Briefly: a solution of PBS containing *gp*51 antigens at a high concentration was directly immobilized on the surface of TiO_2/glass structure. Then the sample was placed into a Petri plate for the incubation in a medium saturated with water vapor at 25 °C. After 10 min of incubation, the surface of the sample was washed with a PBS solution in order to remove not well adsorbed antigens from the surface of TiO_2/glass structure. As a result, a layered structure of *gp*51/TiO_2/glass was formed, which got affinity and selectivity for the one type of bio-molecules – antibodies against leukemia proteins *gp*51 (anti-*gp*51). To prevent a nonspecific interaction (*i.e.*, binding of anti-*gp*51 antibodies directly to unmodified TiO_2 surface), the surface of TiO_2/glass was further treated with a solution of bovine serum albumin (BSA), which after the formation of *gp*51/BSA/TiO_2/glass structure filled still free-remaining sites available for non-specific protein-adsorption standing. Thus it was expected that the selectivity of *gp*51/BSA/TiO_2/glass structure has been improved in comparison to that of BSA-not modified *gp*51/TiO_2/glass structure.

3. Results and discussion

3.1. Interaction of *gp*51 proteins with TiO_2 surface

Proteins consist of amino acids that might contain positively and/or negatively charged radicals that are determining the charge of different protein domains.[21] A large quantity of negatively charged groups such as aldehyde (–CHO), hydroxyl (–OH), carboxyl (–COOH) and positively charged primary amine ($-NH_2$) and some other groups, which are involved into the structure of amino acids, are responsible for the partial (δ+ and δ−) charges of particular protein domains. Therefore the proteins are characterized by electrostatic properties, and sometimes even significant electrostatic 'asymmetry of protein molecule' because the atoms and functional groups, which are forming the protein molecules are charged differently both in charge sign and in absolute charge value. Naturally, the charges in proteins at least partly are compensating each other, but the ternary structure of proteins is relatively rigid and the charged groups have only limited degree of freedom to move within the protein globule. Therefore, in some parts of the protein some uncompensated charge on the surface and inside of the protein still remains.[21] The distribution of charged groups on the surface of the protein depends on the sequence of amino acids, which is pre-determined by the genome that was developed during millions or even billions of years lasting evolution of each protein. During the evolution, the genes which are promoting the synthesis of proteins whose structure the most efficiently matches their function, were selected for further generations.

It should be taken into account that even if the structure of the most proteins is at some extent 'rigid' there is still some degree of flexibility because proteins in their polymeric structure contains a high number of σ-bonds, around which the rotation of protein-building segments is possible. Moreover, both secondary and tertiary structures of the protein are supported by a large number of hydrogen bonds but many of them are not very strong, therefore this factor adds additional degree of freedom for protein structure.[22] The electrostatic interactions, which are based on Coulomb forces between the opposite charges, van der Waals forces and disulfide bonds also play an important role in the formation of both secondary and tertiary structures of protein, but they can be relatively easily disrupted by electrostatic-neutralization and/or displacement of some charged groups/domains, which are forming proteins.

TiO_2 (in its allotropic form of anatase) is a semiconductor of n-type conductivity, usually with an 'upward' band bending of the energy levels when closing the surface of TiO_2 (Fig. 1),[4,6] which indicates the accumulation of a negative charge (bound at surface levels) on its surface.[6,23] The adsorption of the most of

Open Access Article. Published on 09 November 2018. Downloaded on 11/20/2018 8:42:53 AM.
This article is licensed under a Creative Commons Attribution-NonCommercial 3.0 Unported Licence.

molecules is known to introduce an additional charge on the solid state surface and it can change the existing surface energy levels or form the additional ones that are involved in the exchange of charges with the volume of a solid material.[24] It should be taken into account, that in the open air, the oxygen adsorbates (O_{ads}^-) formed on the surface of TiO_2 are resulting in an electron delocalization towards adsorbed oxygen what reduces the conductivity of TiO_2 layer. This process is similar to that, which is well described for ZnO.[25]

Further analysis of the interaction between TiO_2/glass and *gp*51 proteins is based on the evaluation of photoluminescence of TiO_2 nanoparticles. The protein *gp*51 is specifically binding with antibodies against *gp*51 (anti-*gp*51) *i.e.* the target-analyte. The photoluminescence properties of the TiO_2 nanoparticles have been previously investigated in some research papers.[19,20] Moreover, optical effects, which are registered during *gp*51 protein adsorption on TiO_2/glass, also where observed and even applied in the development of photoluminescence based immunosensor for the determination of *gp*51 antibodies.[18,19] However in these publications no attention was paid to the nature of interaction between protein *gp*51 and semiconductor TiO_2 and for the prediction of the mechanism of PL-based signal generation.

In a present research the success of immobilization of *gp*51 and the formation of *gp*51/TiO_2/glass structure was similar to that reported in earlier our works.[19,20] The immobilization of *gp*51 proteins on TiO_2/glass leads to an increase in the intensity of the photoluminescence signal of TiO_2/glass nanostructures and a UV-shift in the position of the maximum of the photoluminescence spectra (Fig. 2a).[19] The application of BSA, which were used to block the free adsorption centers on the TiO_2/glass surface, also leads to a slight increase in the photoluminescence intensity, but the spectrum shift was not observed.

Interaction between *gp*51/TiO_2/glass and anti-*gp*51 leads to the inverse changes in the photoluminescence spectrum (Fig. 2b), *i.e.* a decrease in the integral intensity of the photoluminescence and the IR-shift of spectra. Therefore, the response of the immunosensor *gp*51/TiO_2/glass to anti-*gp*51 can be estimated by two parameters: (i) the photoluminescence intensity and (ii) the position of the PL-maximum. The sensitivity of *gp*51/TiO_2/glass based immunosensor towards anti-*gp*51 was in the range of 2–8 μg ml^{-1}.[19]

3.2. Mechanism of interaction between TiO_2/glass and *gp*51 proteins

A *gp*51 protein molecule has a molecular mass of 51 kDa. The characteristic geometric size of the *gp*51 molecules that are adsorbed on the TiO_2 surface is about 6 nm in diameter.[26] The authors, which have published a research on the formation of *gp*51 protein-based capsid of BLV, have constructed an image of the structure of the *gp*51 protein from the X-ray crystallography data and they have reported that this protein is extra-flexible, which provides very high functionality and the ability to associate and/or dissociate of mainly on *gp*51 protein based the capsid of BLV to/from the membrane of BLV infected cell.[27] Therefore, it is expected that on the surface of TiO_2 *gp*51 protein also forms a well-ordered monolayer. The formation of such layer was confirmed in previous our researches based on the application of spectroscopic ellipsometry.[27–29]

The *gp*51 is not a redox-protein therefore the charge transfer between *gp*51 and TiO_2/glass is not possible.[30] But the *gp*51 protein, like many other proteins, contains a number of partially charged groups and domains, which in Fig. 3 and 4, are represented as partial charges "δ–" and "δ+". These charges per charged atom or group are mostly lower in value than the total single-electron charge (1.6×10^{-19} coulombs). The presence of

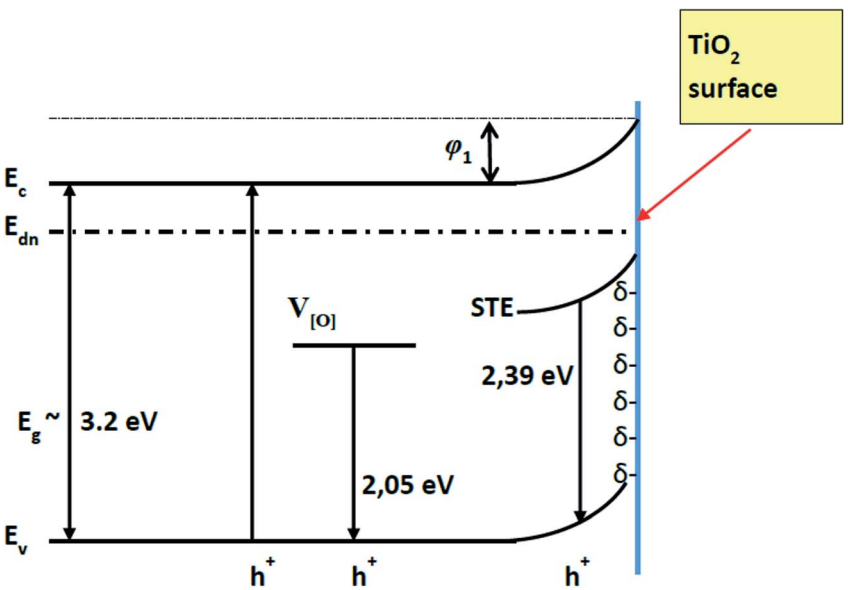

Fig. 1 Energetic levels of pristine TiO_2 (TiO_2/glass structure). E_c, E_v – conduction and valence band of TiO_2 respectively. E_{dn} – electron demarcation level.

 This journal is © The Royal Society of Chemistry 2018

Open Access Article. Published on 09 November 2018. Downloaded on 11/20/2018 8:42:53 AM.
This article is licensed under a Creative Commons Attribution-NonCommercial 3.0 Unported Licence.

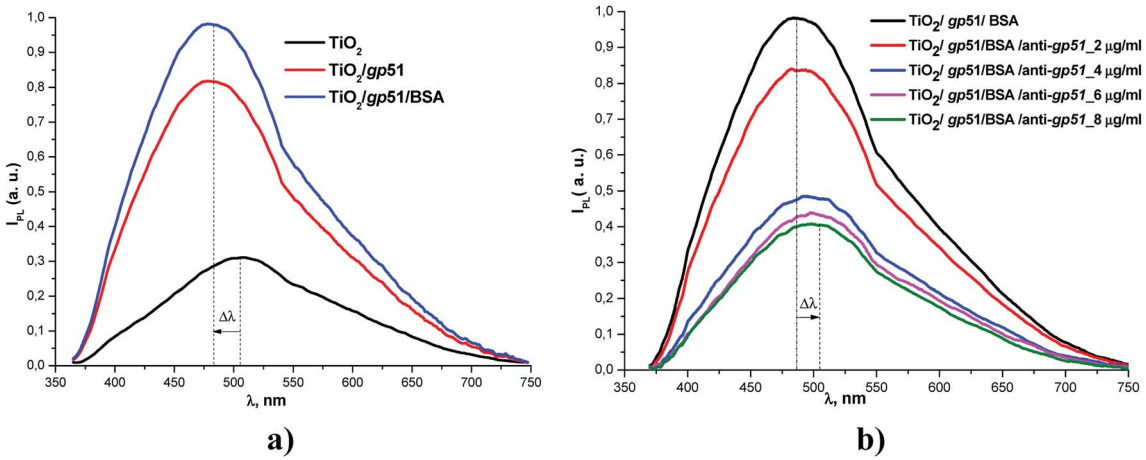

Fig. 2 Photoluminescence spectra of TiO_2/glass nanoparticles: (a) before and after the immobilization of *gp*51 on the TiO_2/glass surface and after BSA deposition; (b) photoluminescence spectra of *gp*51/TiO_2/glass based immunosensor after the interaction with analyte (anti-*gp*51), which is present in the aliquots at different concentrations.

these partial charges suggests that the electrostatic influence of *gp*51 protein on the surface charge of TiO_2/glass is coming from the side of partially uncompensated charges, which are localized in those parts of the *gp*51 protein that are located in close proximity to the surface of TiO_2/glass and are mainly responsible for the adsorption of this protein on the TiO_2/glass surface. The electrostatic Coulomb interaction, which takes place between charged groups in the *gp*51 protein and the negatively charged surface of the TiO_2/glass, are the most strong at a distances ranging from several angstroms to few nanometers. Therefore, among the other interactions such as hydrogen bonds, disulfide bonds, van der Waals interaction, *etc.*, which all also have significant role during the adsorption of proteins, the electrostatic interaction plays one of the most significant role during the adsorption of proteins onto electrically charged surfaces, such as TiO_2. In addition, the local electric fields of charged domains of adsorbed proteins are electrostatically affecting the PL-centers of TiO_2/glass and it causes the shift in the photoluminescence spectra of TiO_2 nanoparticles. Therefore, the photoluminescence maximum of *gp*51/TiO_2/glass, which is mainly caused by self-trapped excitons (STE), shifts from 517 to 499 nm (*i.e.*, to 18 nm), which corresponds to ~0.086 eV that is less than 0.1 eV, and it is one of the proofs of electrostatic interaction based physical adsorption of *gp*51.[24]

The splitting of the photoluminescence spectra into Gaussian curves at each stage of the experiment shows that after

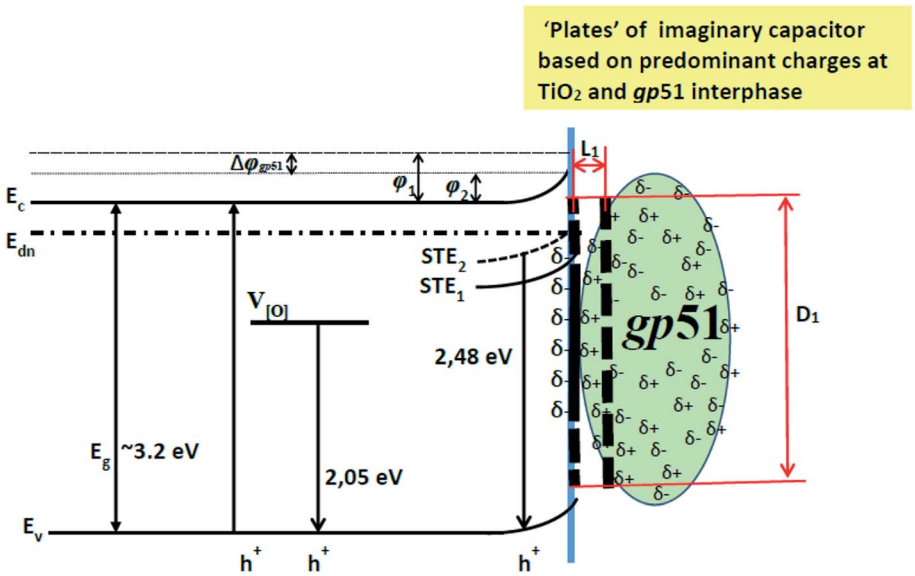

Fig. 3 Energetic levels and the model based on 'imaginary flat capacitor', which represents averaged interaction between charges in *gp*51/TiO_2/glass structure: L_1 – 'relative distance' between 'plates' area of imaginary capacitor, D_2 – diameter of imaginary capacitor, which is determined by surface area of *gp*51 and can be used for the calculation of relative surface area of imaginary capacitor; φ_1 – potential barrier value for surface of TiO_2 interphase with air (air//TiO_2/glass); φ_2 – potential barrier value for *gp*51/TiO_2 structure at interphase with air (air//*gp*51/TiO_2/glass); $\Delta\varphi_{gp51}$ – difference of potential barriers between air//TiO_2/glass and (air//*gp*51/TiO_2/glass) caused by immobilization of *gp*51.

Open Access Article. Published on 09 November 2018. Downloaded on 11/20/2018 8:42:53 AM.
This article is licensed under a Creative Commons Attribution-NonCommercial 3.0 Unported Licence.

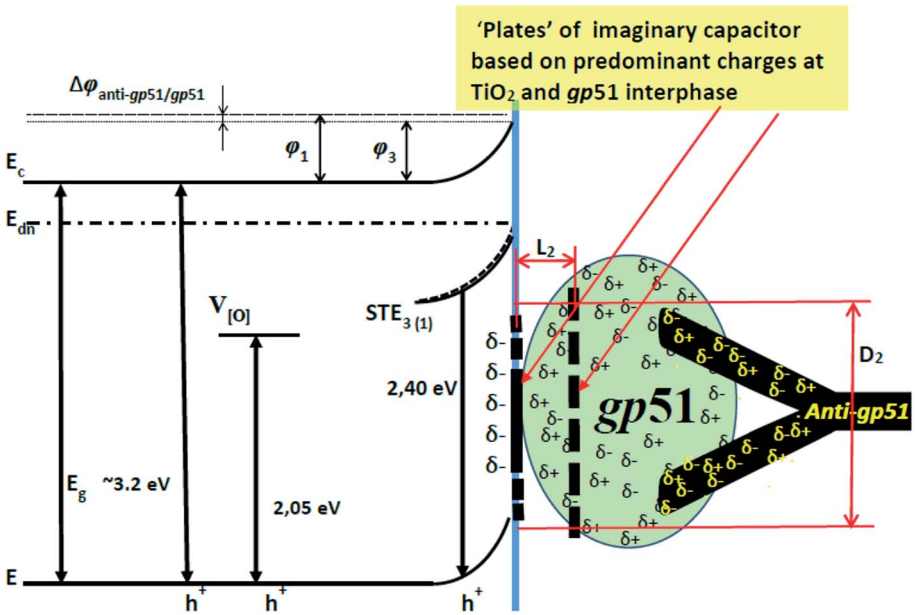

Fig. 4 Energetic levels and the model based on 'imaginary flat capacitor', which represents averaged interaction between charges in anti-gp51/*gp*51/TiO_2/glass structure: L_2 – 'relative distance' between 'plates' area of imaginary capacitor, D_2 – diameter of imaginary capacitor, which is determined by surface area of *gp*51 and can be used for the calculation of relative surface area of imaginary capacitor, φ_3 – potential barrier value for anti-*gp*51/*gp*51/TiO_2/glass structure at interphase with air (air//anti-*gp*51/*gp*51/TiO_2/glass). $\Delta\varphi_{\text{anti-}gp51/gp51}$ – difference of potential barriers between air//TiO_2/glass and air//anti-*gp*51*gp*51/TiO_2/glass.

the adsorption of *gp*51 protein molecules on the TiO_2 surface the energy value of excitation levels, which are responsible for the luminescence and associated with oxygen vacancies $I_{V[O]}$, almost does not change remaining at a value of 605 ± 2 nm. At the same time, the photoluminescence maximum caused by the recombination of STE[31–33] shifts to short wavelengths, changing its position from 517 (I_{STE1} = 2.39 eV) nm to 499 nm (I_{STE2} = 2.48 eV). Since the involvement of the STE level in the process of radiative recombination is regulated by the surface, this indicates that STE level is located either on the surface plane or not very deeply within the surface layer of the TiO_2. The displacement of the light emitting recombination peak indicates that the energy level of STE is complex and has its 'basic' and 'excited' states.[31–33] The appearance of luminescence in the region of 499 nm indicates a radiative transition from the excited STE level. This indicates that the charge at the TiO_2/*gp*51 boundary controls the energy level of the STE and shows that the electronic demarcation level practically coincides with the position of the STE level, *i.e.* is approximately 2.39 eV above the valence band. Therefore, the appearance of proteins on the TiO_2 surface leads to a shift in the energy levels, including energy levels of the light emitting centers, relatively to the electron demarcation level E_{dn}.

The blue-shift of the photoluminescence maximum by 18 nm as a result of adsorption of the *gp*51 protein, which corresponds to $\Delta E_{STE} = STE_2 - STE_1 = 0.086$ eV, also indicates that the initial value of the potential barrier (φ_1) on the TiO_2/glass surface has decreased by a value of 0.086 eV to φ_2. Variation of the potential barrier means that the value of negative charge localized on the TiO_2/glass surface has also changed, due to the charge–charge-based interaction with adsorbed protein *gp*51. Positively charged atoms and groups, which are provided by the *gp*51 protein, partially compensates the surface charge of TiO_2/glass and reduces the energy of electrons localized at the surface levels, which are the most responsible for the generation of PL-signal. Taking into account the fact that the total negative charge predominates on the TiO_2/glass surface, the positively charged parts of the *gp*51 protein electrostatically interact with the negatively charged TiO_2/glass surface. As a result, a partial decrease of the surface charge reduces the electric field in the TiO_2/glass surface region. Further interaction of *gp*51/TiO_2/glass structure with analyte – anti-*gp*51, which is also a protein, leads to the inverse changes in the photoluminescence spectra, *i.e.*, to UV-shift of the spectrum and decrease the photoluminescence intensity to the value that corresponds to the pure TiO_2/glass. The latter effect is based on the formation of an immune complex between immobilized antigens *gp*51 and anti-*gp*51 antibodies, which are present in aliquot. The formation of this immune complex besides the van der Waals interaction and other interactions at a very high extent is based on the interaction between oppositely charged domains, functional groups and atoms in *gp*51 and anti-*gp*51 molecules (including the formation of number of hydrogen bounds, which can be estimated as specific kind of electrostatic interaction). It can be assumed that uncompensated charges (δ+ and δ) of both proteins (*gp*51 and anti-*gp*51) are involved in electrostatic interactions during the formation of immune complex. As a result, some of the charged groups of protein *gp*51 that were originally involved in the interaction between *gp*51 and TiO_2/glass are at least partially compensated by the opposite charge of the anti-*gp*51 protein groups, thereby reducing the direct electrostatic effect from immobilized *gp*51 proteins to the

 This journal is © The Royal Society of Chemistry 2018

Open Access Article. Published on 09 November 2018. Downloaded on 11/20/2018 8:42:53 AM.
This article is licensed under a Creative Commons Attribution-NonCommercial 3.0 Unported Licence.

charged surface of TiO_2 and at the same time to PL-light emitting centers.

The effects described above have an effect on the shift of PL-maximum and on the decrease in the potential barrier on *gp*51/TiO_2/glass interface due to the charge–charge interaction between TiO_2/glass and *gp*51. The potential barrier at the interface between TiO_2/glass and *gp*51 has a greater value in *gp*51/TiO_2/glass structure in comparison with that in anti-*gp*51/*gp*51/TiO_2/glass due to partial compensation (decrease in value) and/or delocalization of *gp*51 charges, which were initially involved into interaction between TiO_2/glass and *gp*51 after formation of *gp*51/TiO_2/glass structure.

The changes in the PL intensity from TiO_2 after the protein adsorption can be caused by following reasons. An increase of the PL intensity after immobilization of *gp*51 proteins on the TiO_2/glass surface could result from the fact that the oxygen, adsorbed on the surface of TiO_2, forms a re-oxidized layer that is reduced by the atoms and groups in *gp*51 proteins. A decrease of the PL intensity after the interaction of biosensitive layer with the target analyte can be caused by both additional dispersion of light from the excitation source and exited PL signal generated from anti-*gp*51/gp51/TiO_2/glass structure.

The distribution of charges in *gp*51/TiO_2/glass structure can also be interpreted as a model based on an 'imaginary capacitor' (Fig. 3), formed as a result of the electrostatic interaction between oppositely charged protein *gp*51 layer and the TiO_2/glass surface. The 'imaginary capacitor' is formed as a result of protein *gp*51 adsorption on TiO_2/glass surface, after which the charges are distributed in energetically most favorable way, partially compensating each other. Consequently, the positive 'imaginary capacitor plate' is based on the positive charges, which are predominant in the protein *gp*51 surface area that after adsorption appears in close proximity to *gp*51/TiO_2/glass interface and/or due to the negative electrostatic effect of TiO_2/glass are induced/attracted closer to negatively charged TiO_2/glass surface.

Charged atoms/groups/domains of *gp*51 that are localized in the close proximity to the TiO_2/glass surface and they electrostatically affect the TiO_2 emission centers and the energy value of the surface potential barrier. Thus the position of the energy levels of the TiO_2/glass emission maximum depends on TiO_2 surface modification stage (TiO_2/glass or *gp*51/TiO_2/glass) shifts from/backwards the initial position of the demarcation level. Fig. 3 represents an imaginary capacitor consisting of a negatively charged plate on the surface of TiO_2/glass and an 'imaginary positively charged plate' formed in *gp*51 protein in close proximity to *gp*51/TiO_2/glass interphase.

Hence, the interaction of *gp*51/TiO_2/glass with anti-*gp*51 antibodies and the formation of *gp*51/anti-*gp*51-based immune complex leads to a 'deformation' and the reduction of charge 'stored' on 'the positive imaginary capacitor plate' (Fig. 4). This is mainly due to the redistribution and partial compensation of charges during the formation of the *gp*51/anti-*gp*51 immune complex, which in turn reduces the charge of 'the imaginary capacitor plate' based on *gp*51 ($q_2 < q_1$). This reduced charge can be interpreted as the reduction of the area of the same plate (S_2) and/or the increase of the distance (d_2) between the two imaginary capacitor plates based on *gp*51 and TiO_2/glass. This effect is observed because some of the *gp*51 protein charges move from the *gp*51/TiO_2/glass interface towards interacting anti-*gp*51 protein and are partially compensated by charge present in anti-*gp*51, whereby the imaginary positive *gp*51-based capacitor plate of the capacitor is reduced in imaginary surface area and/or correspondingly moving apart from the negative TiO_2/glass plate. This effect leads to a decrease in the capacitance of this imaginary capacitor and the electric field induced by *gp*51 becomes reduced. Therefore, after the interaction of *gp*51/TiO_2/glass with anti-*gp*51 antibodies and the formation of *gp*51/anti-*gp*51 complex, which is involved into anti-*gp*51/*gp*51/TiO_2/glass structure, the electrostatic effect of *gp*51 initially adsorbed on TiO_2/glass towards the TiO_2 surface significantly decreases.

It should be taken into account that after the adsorption of *gp*51 proteins, the oppositely charged domains build up within a surface layers of both adsorbed-*gp*51 and TiO_2/glass within the Debye-screening length of both materials. These oppositely charged electric layers forms a double-layered structure with obvious electric capacitance that is dependent on (i) the concentration of charged atoms/groups/domains, (ii) distance of these features from each other and dielectric constant (relative permittivity) of *gp*51 and space in between adsorbed *gp*51 and TiO_2/glass. Any charge that is emerging within the Debye-screening length on the surfaces of both adsorbed-*gp*51 and TiO_2/glass is affecting the capacitance of this imaginary capacitor. The variation of both (i) the number and (ii) the localization of charged parts depends on so called 'Debye-screening length' towards all directions of structures and influences the strength of electric field in *gp*51/TiO_2/glass and anti-*gp*51/*gp*51/TiO_2/glass structures. The relationships among the value of the Debye-screening length (L_D) and the concentration of charged atoms/groups/domains of *gp*51 are provided in eqn (1) and/or (2):

$$L_D = \sqrt{\frac{\varepsilon\varepsilon_0 kT}{2ne^2}} \quad (1)$$

where: ε_0 is the permittivity (dielectric constant of vacuum) in vacuum, ε is the permittivity (dielectric constant) of the TiO_2 (or the relative permittivity of *gp*51 protein if Debye-screening length is calculated for *gp*51 protein), T is the absolute temperature (in kelvin), n is the concentration of the electrons, e is the electron charge.

$$k^{-1} = \sqrt{\frac{\varepsilon\varepsilon_r k_B T}{2N_A e^2 I}} \quad (2)$$

where: I is the concentration of charged atoms/groups/domains of the *gp*51 protein (mol m^{-3}), k_B is the Boltzmann constant, T is the absolute temperature (in kelvin), ε_r is the relative permittivity of *gp*51 protein, N_A is the Avogadro number, e is the 'averaged elementary charge of electron' and k is the Debye–Hückel screening length in TiO_2 or in *gp*51 protein, which is strongly dependent on the concentration (N_d) of charged 'defects' in TiO_2 or atoms/groups/domains or in *gp*51 protein, respectively. In this context it should be noted that if Debye-

Open Access Article. Published on 09 November 2018. Downloaded on 11/20/2018 8:42:53 AM.
This article is licensed under a Creative Commons Attribution-NonCommercial 3.0 Unported Licence.

screening length is calculated for *gp*51 protein then 'averaged elementary charge' can vary between elementary charge of electron 1.6×10^{-19} Cb and 0 due to variety of possible δ+ and δ–, which are appearing within protein globule. It should be also noted that the exact concentrations of charged atoms or impurities, which is relatively easily calculated for TiO_2, but it is no case for proteins such as *gp*51 where exact number of charged atoms/groups/domains is not always known and can vary dependably on conformation of protein. Therefore this value should be calculated from the combination of other measurements such as electrochemical impedance spectroscopy,[34] *etc.*

Debye-screening length for TiO_2, calculated according to the eqn (1), while applying such values ε – permittivity in TiO_2 ($\varepsilon = 34$),[35] ε_0 – dielectric constant (8.85×10^{-12} F m^{-1}), n – concentration of electrons in TiO_2 ($n = 10^{19}$ sm^{-3}), e – electron charge (1.6×10^{-19} Cb), k – Boltzmann's constant (1.38×10^{-23} J K^{-1}) and T – absolute temperature (293 K) was estimated to be 15 nm. The estimated value of L_D shows that within this distance from TiO_2 surface the PL-centres are affected by electrostatic effects from adsorbed proteins *gp*51 and anti-*gp*51/*gp*51.

The measured PL-peak values determine how the concentration and distribution of charged atoms/groups/domains charge density affect the TiO_2 surface potential and potential of energetic levels within Debye-screening length, which can be determined using eqn (1) and (2). This effect is similar to that observed on field effect transistors.[36–38] The sensitivity of TiO_2-based PL immunosensor is also influenced by the concentration and distribution of charged atoms/groups/domains (Debye-screening length) in protein *gp*51 or gp51/anti-gp51-based immune-complex.

4. Conclusions

The main aspects of the interaction mechanism between nanostructured TiO_2/glass layer and bovine leukemia virus proteins *gp*51, during the formation of PL-based immunosensor, have been outlined. Bovine leukemia virus protein *gp*51, which was adsorbed on the surface of nanostructured TiO_2/glass thin film, formed the biosensitive layer (*gp*51/TiO_2/glass) that resulted in the TiO_2 PL peak shift from 517 nm to 499 nm. The interaction *gp*51/TiO_2/glass structure with specific antibodies against *gp*51 (anti-*gp*51) has shifted the PL peak backwards from 499 nm to 516 nm. These PL shifts are attributed to the variation of STE energy level, which was induced by changes of electrostatic interaction between adsorbed *gp*51 and negatively charged TiO_2/glass surface. The displacement of the light emitting recombination peak confirms that the energy of STE level is complex and has its ground and excited states. The blue-shift of the photoluminescence maximum by 18 nm as a result of adsorption of the *gp*51 protein, which corresponds to $\Delta E_{STE} = I_{STE2} - I_{STE1} = 0.086$ eV, indicates that the initial value of the potential barrier on the TiO_2/glass surface has decreased by 0.086 eV. The variation of the potential barrier means that the value of negative charge localized on the TiO_2/glass surface has changed due to the charge–charge-based interaction with adsorbed protein *gp*51. Positively charged atoms and groups, provided by the *gp*51 protein, partially compensate the surface charge of TiO_2 and reduce the energy of electrons localized at the surface levels, which are the most responsible for the generation of PL-signal.

The charge–charge-based interaction in the double charged layers *gp*51/TiO_2/glass can also be interpreted as a model based on 'imaginary capacitor', formed as a result of the electrostatic interaction between oppositely charged protein *gp*51 layer and the TiO_2/glass surface. The positive charges of protein *gp*51, attracted to the negatively charged surface, form the positive 'imaginary capacitor plate' in the close proximity to *gp*51/TiO_2/glass interface. The interaction of *gp*51/TiO_2/glass with anti-*gp*51 antibodies and formation of *gp*51/anti-*gp*51-based immune complex leads to a deformation and reduction of charge in 'the positive imaginary capacitor plate', caused by redistribution and partial compensation of charges during the formation of the *gp*51/anti-*gp*51 immune complex. Debye-screening length, calculated for TiO_2, is in the range of 15 nm, which shows that PL-centres within this distance can be electrostatically affected by adsorbed *gp*51 and anti-*gp*51/*gp*51 complex.

The highlighted origin of the changes in the photoluminescence spectra of TiO_2 as a result of the formation of biosensitive layer and after its interaction with the analyte, bring us closer to an understanding of the interaction mechanism between TiO_2 and proteins, that is the key in the solving of many issues related to an improvement of biosensor performance.

In our next work we are going to investigate more in detail some parts of here predicted interaction mechanism using other proteins adsorbed on the surface of TiO_2/glass.

Conflicts of interest

There are no conflicts to declare.

Acknowledgements

This research was supported by Ukrainian-Lithuanian Research project "Application of hybrid nanostructures which are based on TiO_2 or ZnO and modified by biomolecules, in optoelectronic sensors" Lithuanian Research Council project No. P-LU-18-53.

References

1 A. Ramanaviciene and A. Ramanavicius, Molecularly imprinted polypyrrole-based synthetic receptor for direct detection of bovine leukemia virus glycoproteins, *Biosens. Bioelectron.*, 2004, **20**, 1076–1082.
2 B. Kurtinaitiene, D. Ambrozaite, V. Laurinavicius, A. Ramanaviciene and A. Ramanavicius, Amperometric immunosensor for diagnosis of BLV infection, *Biosens. Bioelectron.*, 2008, **23**, 1547–1554.
3 A. Tereshchenko, M. Bechelany, R. Viter, V. Khranovskyy, V. Smyntyna, N. Starodub and R. Yakimova, Optical

 This journal is © The Royal Society of Chemistry 2018

Open Access Article. Published on 09 November 2018. Downloaded on 11/20/2018 8:42:53 AM.
This article is licensed under a Creative Commons Attribution-NonCommercial 3.0 Unported Licence.

biosensors based on ZnO nanostructures: advantages and perspectives, *Sens. Actuators, B*, 2016, **229**, 664–677.

4 S. M. Gupta and M. Tripathi, A review of TiO_2 nanoparticles, *Chin. Sci. Bull.*, 2011, **56**, 1639–1657.

5 Z. Bian, J. Zhu, Y. Huo, H. Li and Li Y. Lu, Mesoporous Au/TiO_2 Nanocomposites with Enhanced Photocatalytic Activity Hexing, *J. Am. Chem. Soc.*, 2007, **129**(15), 4538–4539.

6 H. Xu, P. Reunchan, S. Ouyang, H. Tong, N. Umezawa, T. Kako and J. Ye, Anatase TiO_2 Single Crystals Exposed with High-Reactive {111} Facets Toward Efficient H_2 Evolution, *Chem. Mater.*, 2013, **25**(3), 405–411.

7 J. Liu, D. Olds, R. Peng, L. Yu, G. S. Foo, Sh. Qian, J. Keum, B. S. Guiton, Z. Wu and K. Page, Quantitative Analysis of the Morphology of {101} and {001} Faceted Anatase TiO_2 Nanocrystals and Its Implication on Photocatalytic Activity, *Chem. Mater.*, 2017, **29**(13), 5591–5604.

8 Y. Zhou, H. Wang, Y. Zhuo, Y. Chai and R. Yuan, Highly Efficient Electrochemiluminescent Silver Nanoclusters/Titanium Oxide Nanomaterials as a Signal Probe for Ferrocene-Driven Light Switch Bioanalysis, *Anal. Chem.*, 2017, **89**(6), 3732–3738.

9 Y. Li, S. Zhanga, H. Dai, Z. Hong and Y. Lin, An enzyme-free photoelectrochemical sensing of concanavalin A based on graphene-supported TiO_2 mesocrystal, *Sens. Actuators, B*, 2016, **232**, 226–233.

10 J. Qiu, S. Zhang and H. Zhao, Recent applications of TiO_2 nanomaterials in chemical sensing in aqueous media, *Sens. Actuators, B*, 2011, **160**(1), 875–890.

11 Y.-M. Chu, C.-C. Lin, H.-C. Chang, C. Li and C. Guo, TiO_2, nanowire FET device: Encapsulation of biomolecules by electro polymerized pyrrole propylic acid, *Biosens. Bioelectron.*, 2011, **26**, 2334–2340.

12 K.-S. Mun, S. D. Alvarez, W.-Y. Choi and M. J. Sailor, A Stable, Label-free Optical Interferometric Biosensor Based on TiO_2 Nanotube Arrays, *ACS Nano*, 2010, **4**, 2070–2076.

13 S. Rajendran, D. Manoj, K. Raju, D. D. Dionysiou, M. Naushad, F. Gracia, L. Cornejo, M. A. Gracia-Pinilla and T. Ahamad, Influence of mesoporous defect induced mixed-valent NiO (Ni^{2+}/Ni^{3+})-TiO_2 nanocomposite for non-enzymatic glucose biosensors, *Sens. Actuators, B*, 2018, **264**, 27–37.

14 T. Zheng, E. Feng, Z. Wang, X. Gong and Y. Tian, Mechanism of Surface-Enhanced Raman Scattering Based on 3D Graphene–TiO_2 Nanocomposites and Application to Real-Time Monitoring of Telomerase Activity in Differentiation of Stem Cells, *ACS Appl. Mater. Interfaces*, 2017, **9**(42), 36596–36605.

15 A. Tereshchenko, V. Fedorenko, V. Smyntyna, I. Konup, A. Konup, M. Eriksson, R. Yakimova, A. Ramanavicius, S. Balme and M. Bechelany, ZnO films formed by atomic layer deposition as an optical biosensor platform for the detection of Grapevine virus A-type proteins, *Biosens. Bioelectron.*, 2017, **92**, 763–769.

16 R. Plugaru, A. Cremades and J. Piqueras, The effect of annealing in different atmospheres on the luminescence of polycrystalline TiO_2, *J. Phys.: Condens. Matter*, 2004, **16**, S261–S268 PII: S0953-8984(04) 67008-1.

17 J. Preclíková, P. Galář, F. Trojánek, S. Daniš, B. Rezek, I. Gregora, Y. Němcová and P. Malý, Nanocrystalline titanium dioxide films: Influence of ambient conditions on surface- and volume-related photoluminescence, *J. Appl. Phys.*, 2010, **108**, 113502.

18 R. Viter, A. Tereshchenko, V. Smyntyna, N. Starodub, R. Yakimova, V. Khranovskyy and A. Ramanavicius, Toward development of optical biosensors based on photoluminescence of TiO_2 nanoparticles for the detection of Salmonella, *Sens. Actuators, B*, 2017, **252**, 95–102.

19 R. Viter, V. Smyntyna, N. Starodub, A. Tereshchenko, A. Kusevitch, I. Doycho, S. Geveluk, N. Slishik, J. Buk, J. Duchoslav, J. Lubchuk, I. Konup, A. Ubelis and J. Spigulis, Novel Immune TiO_2 Photoluminescence Biosensors for Leucosis Detection, *Procedia Eng.*, 2012, **47**, 338–341.

20 R. Viter, N. Starodub, V. Smyntyna, A. Tereschenko, A. Kusevitch, J. Sitnik, J. Buk and J. Macak, Immune biosensor based on Silica Nanotube Hydrogels for rapid Biochemical Diagnostics of Bovine Retroviral Leukemia, *Procedia Eng.*, 2011, **25**, 948–951.

21 D. L. Nelson, M. M. Cox and A. L. Lehninger, *Principles of Biochemistry*, Worth Publishtrs Inc., New York, 2000.

22 V. Shewale, P. Joshi, S. Mukhopadhyay, M. Deshpande, R. Pandey, S. Hussain and S. Karna, First-principles study of nanoparticle-biomolecular interactions: anchoring of a $(ZnO)_{12}$ cluster on nucleobases, *J. Phys. Chem.*, 2011, **115**, 10426–10430.

23 M. C. Wu, A. Sapi, A. Avila, M. Szabó, J. Hiltunen, M. Huuhtanen, G. Tóth, Á. Kukovecz, Z. Kónya, R. Keiski, W.-F. Su, H. Jantunen and K. Kordás, Enhanced photocatalytic activity of TiO_2 nanofibers and their flexible composite films: decomposition of organic dyes and efficient H_2 generation from ethanol–water mixtures, *Nano Res.*, 2011, **4**(4), 360–369.

24 V. Smyntyna *Electron and Molecular Phenomena on the Surface of Semiconductors*, Nova Publishers, New York, 2013, p. 208.

25 S. G. Ansari, R. Wahab, Z. A. Ansari, Y. S. Kim, G. Khang, A. Al-Hajry and H. S. Shin, Effect of nanostructure on the urea sensing properties of sol–gel synthesized ZnO, *Sens. Actuators, B*, 2009, **137**, 566–573.

26 G. Obal, F. Trajtenberg, F. Carrión, L. Tomé, N. Larrieux, X. Zhang, O. Pritsch and A. Buschiazzo, Conformational plasticity of a native retroviral capsid revealed by X-ray crystallography, *Science*, 2015, **5182**, 1–7.

27 Z. Balevicius, I. Baleviciute, S. Tumenas, L. Tamosaitis, A. Stirke, A. Makaraviciute, A. Ramanaviciene and A. Ramanavicius, In situ study of ligand-receptor interaction by total internal reflection ellipsometry, *Thin Solid Films*, 2014, **571**, 744–748.

28 I. Baleviciute, Z. Balevicius, A. Makaraviciute, A. Ramanaviciene and A. Ramanavicius, Study of Antibody/Antigen Binding Kinetics by Total Internal Reflection Ellipsometry, *Biosens. Bioelectron.*, 2013, **39**, 170–176.

29 Z. Balevicius, A. Makaraviciute, G. J. Babonas, S. Tumenas, V. Bukauskas, A. Ramanaviciene and A. Ramanavicius, Study of optical anisotropy in thin molecular layers by

Open Access Article. Published on 09 November 2018. Downloaded on 11/20/2018 8:42:53 AM.
This article is licensed under a Creative Commons Attribution-NonCommercial 3.0 Unported Licence.

total internal reflection ellipsometry, *Sens. Actuators, B*, 2013, **181**, 119–124.

30 T. Ogawa *Biochemistry, Genetics and Molecular Biology: 'Protein Engineering - Technology and Application'*, 2013, ISBN 978-953-51-1138-2, DOI: 10.5772/56265.

31 M. C. Fravventura, L. D. A. Siebbeles and T. J. Savenije, Mechanisms of Photogeneration and Relaxation of Excitons and Mobile Carriers in Anatase TiO_2, *J. Phys. Chem. C*, 2014, **118**, 7337–7343.

32 I. Sildos, A. Suisalu, V. Kiisk, M. Schuisky, H. Mändar, T. Uustare and J. Aarik, Effect of Structure Development on Self-Trapped Exciton Emission of TiO_2 Thin Films, *Proc. SPIE*, 2000, **4086**, 427–430.

33 K. Wakabayashi, Y. Yamaguchi, T. Sekiya and S. Kurita, Time-resolved luminescence spectra in colorless anatase TiO_2 single crystal, *J. Lumin.*, 2005, **112**, 50–53.

34 A. Ramanavicius, A. Finkelsteinas, H. Cesiulis and A. Ramanaviciene, Electrochemical impedance spectroscopy of polypyrrole based electrochemical immunosensor, *Bioelectrochemistry*, 2010, **7**, 11–16.

35 H. Tang, K. Prasad and R. Sanjinbs, Electrical and optical properties of TiO_2 anatase thin films, *J. Appl. Phys.*, 1994, **75**(4), 2042–204.

36 Z. Li, Y. Chen, X. Li, T. I. Kamins, K. Nauka and R. S. Williams, Encoding Information in DNA: From Basic Structure to Nanoelectronics, *Nano Lett.*, 2004, **4**, 245–247.

37 E. Stern, R. Wagner, F. J. Sigworth, R. Breaker, T. M. Fahmy and M. A. Reed, Importance of the Debye Screening Length on Nanowire Field Effect Transistor Sensors, *Nano Lett.*, 2007, **7**(17), 3405–3409.

38 G. Zheng, F. Patolsky, Y. Cui, W. U. Wang and C. M. Lieber, Multiplexed electrical detection of cancer markers with nanowire sensor arrays, *Nat. Biotechnol.*, 2005, **23**, 1294–1301.

This journal is © The Royal Society of Chemistry 2018